Original Research Article

Modelling and Estimating Photosynthetically Active Radiation from Measured Global Solar Radiation at Calabar, Nigeria.

Abstract

In this research paper, measured monthly average daily radiometric data for global solar radiation on the horizontal surfaces and atmospheric parameters including relative humidity, sunshine hours, dew point temperature as well as the ambient temperatures (minimum and maximum) at Calabar, Nigeria obtained from the archives of the Nigeria Meteorological Agency, Oshodi Lagos, Nigeria for a 14-year period (2000-2013) were analysed and fifteen empirical models developed for predicting photosynthetically active radiation (PAR) for Calabar environment. The photosynthetically active radiation is estimated from measured global while the models are developed using extraterrestrial PAR, relative humidity, relative sunshine hours, dew point temperature as well as the relative ambient temperature (minimum and maximum) and clearness index. The performance of the models developed were tested for validation using mean bias error (MBE), root mean square error (RMSE), mean percentage error (MPE), Nash-Sutcliff equation (NSE), chi squares (χ^2) and index of agreement (d). the linear, quadratic and polynomial regression models developed to estimate PAR judging from the model performance and validation test indicates that the proposed models could be used to estimate PAR in Calabar environ and other locations with similar climatological conditions across the globe.

***Keywords*:** Atmospheric Parameters; Calabar; Clearness Index; Global Solar Radiation; Modelling; Photosynthetically Active Radiation

1. Introduction

Photosynthetically active radiation (PAR) is the light wavelength range that is best fit for photosynthesis to occur. Photosynthesis is a process that requires light energy and optimally occurs within the broad range of broad bandwave of 400-700nm [1, 2]. The range is also within the visible light. Visible light encompasses the electromagnetic spectrum from visible blue/violet to red. Blue light has a higher energy and shorter wavelength than green or red light, while red light has the lowest energy in the visible spectrum.

Photons at shorter wavelengths tend to be so energetic that they can be damaging to cells and tissues but are mostly filtered out by the ozone layer in the stratosphere while photons with longer wavelengths do not carry enough energy to allow photosynthesis to take place McCree [1]. In general, plants use PAR as an energy source to convert carbon IV oxide (CO_2) and water (H_2O) through photosynthesis into organic compounds (typically sugar, called glucose) which are then used to synthesize structural and metabolic energy required for plant growth and development, respiration, as well as stored vegetative products that result in plant biomass. This can be stated in a more convenient form as:

$$6CO_{2(liquid)} + 12H_2O_{(liquid)} + \text{Photon} \rightarrow C_6H_{12}O_{6(aqueous)} + 6O_{2(gas)} + 6H_2O_{(liquid)} \quad (1)$$

The photon in equation (1) is known as PAR. This component of solar radiation spectrum (PAR) is extremely essential, because it is the solar energy source for vegetative photosynthesis to provide us with products such as food and fibre sources, biofuel carriers and additional material sources that support industrial process. It also plays very important roles in plant growth, and it is the principal factor in the rate of solar energy conversion into biological mediated energy. Proper prediction and understanding of this radiometric parameter (PAR) are needed for numerous applications, such as studies of radiation climate, remote sensing of vegetation, radiation regimes of plant canopy and photosynthesis, an essential input in models estimating plant productivity, and carbon exchange between ecosystem and atmosphere.

Measurements of PAR have been performed in many parts of the world using a variety of techniques. These techniques involve the use of Eppley precision spectral pyranometer (PSP), Li-COR quantum sensors (Li-190SZ) and PAR lite. Unfortunately, a worldwide routine network for the measurement of PAR is not yet established. In order to circumvent this problem, Williams [3] conducted a simulation for a wide variety of climatic conditions and concluded that the ratio of PAR to global solar radiation (SR) is constant. PAR to SR has been investigated worldwide to predict PAR from routine measured SR, and on the basis of previous studies in several locations, PAR to SR basically falls between 0.45 and 0.50, as shown in Tsubo and Walker [4]. Moon [5] computed the spectral distribution of direct sunlight for sea level and suggested that PAR/SR was between

44% and 45% at places of low altitudes when the sun was more than 30° above the horizon, while Monteith [6] suggested that the PAR can be taken as half of the total SR in the tropics as well as in temperate latitudes based on his measurement at Sutton Bonington (52°N, 50°W). Howell et al. [7] and Meek et al. [8] estimated PAR to be 45% of SR. Several studies have observed that PAR varied according to location [4, 9, 10], Sky conditions [11, 12], sky clearness, sky brightness and atmospheric depth for the solar beam [13], relative sunshine duration and water vapor pressure [14], altitude [15], irradiance intensity [16], day length [17, 16], dust and aerosol [18], pyrogenic aerosols from biomass burning [10], atmospheric transmittance includes the attenuation of solar radiation by dust and aerosol scattering, and absorption by water, ozone and other atmospheric gases [19, 13, 20]. It is therefore imperative to develop a set of models for estimating PAR from the measured SR and other meteorological parameters enumerated by these researchers that will conveniently estimate the influence of atmospheric conditions on this radiometric parameter. This will produce amount of appreciated PAR data without the substantial cost of the instrumentation network that would otherwise be needed. The aim of this paper is to develop empirical models for estimating PAR from global solar radiation data in Calabar, Nigeria and other geographical locations with similar climatological conditions.

2. Materials and Methods

The site considered in this study is Calabar, Nigeria, located on latitude $04^{o}71^{1}$ N and longitude $08^{o}55^{1}$ E and 62.3m above sea level. The monthly average daily data for global solar radiation on horizontal surfaces, relative humidity, sunshine hours, dew point temperature as well as the ambient temperatures (minimum and maximum) were obtained from the archives of the Nigeria Meteorological Agency, Oshodi Lagos, Nigeria for a 14-year period (2000-2013). The global solar radiation data obtained using Gunn-Bellani radiation integrators were converted to $MJm^{-2}day^{-1}$ using the conversion 1ml is equivalent to 1.216 $MJm^{-2}day^{-1}$ Ododo [21].

2.1 Model Development

Various measuring techniques and climatic parameters have been used in developing empirical models for estimating PAR. In this paper, the constant ratio of 45% of measured global solar radiation data as generalized by several researchers [5, 3, 7, 8, 4, 14] was used to obtain the PAR data since there is no standard weather station that routinely measure PAR in Calabar. Therefore, PAR can estimated mathematically thus:

$$PAR = 0.45\overline{H} \tag{2}$$

Where $\overline{H}$ is the measured global solar radiation the horizontal surface. The extraterrestrial solar radiation on the horizontal surface $\overline{H}_O$, is given by Iqbal [22] as follow:

$$H_O = \frac{24}{\pi} I_{SC} E_o \left[\frac{\pi}{180} \omega_s \sin\phi \sin\delta + \cos\phi \cos\delta \sin\omega_s \right] \tag{3}$$

Where I_{SC} is the solar constant, E_O is the eccentricity correction factor, ϕ is the latitude of the location, δ is the solar declination and ω_s is the hour angle. The expression for I_{SC}, E_O, ϕ, δ and ω_s are given by Liou [23] as:

$$I_{SC} = \frac{1367 \times 3600}{1000000} (MJm^{-2}h^{-1}) \tag{4}$$

$$E_O = 1 + 0.033 \cos\left(\frac{360N}{365} \right) \tag{5}$$

Where N is the characteristics day number for each month as shown in table 1.

$$\delta = 23.45 Sin\left[\frac{360(N + 284)}{365} \right] \tag{6}$$

$$\omega_s = Cos^{-1}\left(-\tan\phi \tan\delta \right) \tag{7}$$

The average day length for each month was collected using the expression by [23] as:

$$\overline{S}_o = \frac{2}{15} Cos^{-1}\left(-\tan\phi \tan\delta \right) \tag{8}$$

The extraterrestrial PAR was estimated as 40% of the extraterrestrial global solar radiation as generalized by Monteith and Unsworth [19]. It was assumed that the sun-earth distance did not vary seasonally because the ratio of the distance between the earth and the sun on a specific day to the mean distance throughout the year is never more than 3.5% away from one Gates [24]. Thus, extraterrestrial photosynthetically active radiation, PAR_O, can expressed and estimated as:

$$PAR_O = 0.4\overline{H}_o \tag{9}$$

The monthly mean daily values of PAR on the horizontal surface was correlated with the monthly mean daily values of the relative humidity, relative sunshine hours, extraterrestrial global solar radiation, extraterrestrial PAR, dew point temperature as well as the relative ambient temperatures (minimum and maximum), to generate fifteen models (linear, quadratic and polynomial equations) which were used to estimate the PAR at Calabar. A computer statistical software program (IBM SPSS 20) was used in obtaining the regression constants, correlation coefficient (R), coefficient of determination (R^2) and adjusted coefficient of determination (R^2). The performance of the models were tested by calculating Nash-Sutcliff equation (NSE), chi square (χ^2) and index of agreement (d). However, the error in the prediction were evaluated by the mean bias error (MBE), root mean square error (RMSE), mean percentage error (MPE). The PAR predicted (model) and observed values were plotted against the months of the year to observe how well the predictive (model) values fit in with the observed PAR values. Therefore, the sets of models developed for estimating PAR at Calabar, Nigeria are given as:

Model 1: $$\frac{PAR}{\overline{H}_o} = 0.001 + 0.448Kt \tag{10}$$

Model 2: $$\frac{PAR}{\overline{H}_o} = 0.009 + 0.406Kt + 0.050Kt^2 \tag{11}$$

Model 3: $$\frac{PAR}{\overline{H}_o} = -0.002 + 0.448Kt + 0.004\frac{\overline{s}}{\overline{S}_o} \tag{12}$$

Model 4: $$\frac{PAR}{PAR_o} = 0.002 + 1.119Kt \tag{13}$$

Model 5: $$\frac{PAR}{PAR_o} = 0.020 + 1.034Kt + 0.103Kt^2 \tag{14}$$

Model 6: $$\frac{PAR}{PAR_o} = -0.003 + 1.120Kt + 0.007\frac{\overline{s}}{\overline{S}_o} \tag{15}$$

Model 7: $$\frac{PAR}{PAR_o} = 0.005 - 0.002\frac{\overline{R}}{100} + 1.118Kt \tag{16}$$

Model 8: $$\frac{PAR}{PAR_o} = 0.253 - 0.022\frac{\overline{R}}{100} + 1.326Kt^2 \tag{17}$$

Model 9: $$\frac{PAR}{PAR_o} = 0.025 - 0.003\frac{\overline{R}}{100} + 1.025Kt + 0.111Kt^2 \tag{18}$$

Model 10: $$\frac{PAR}{PAR_o} = 0.001 - 0.008\frac{\overline{R}}{100} + 0.014\frac{\overline{s}}{\overline{S}_o} + 1.114Kt \tag{19}$$

Model 11: $$\frac{PAR}{PAR_o} = 0.002 + 0.003\frac{\overline{T}_{dew}}{100} + 1.120Kt \tag{20}$$

Model 12: $$\frac{PAR}{PAR_o} = -0.008 + 0.016\frac{\overline{T}_{dew}}{100} + 0.009\frac{\overline{s}}{\overline{S}_o} + 1.121Kt \tag{21}$$

Model 13: $$\frac{PAR}{\overline{H}_o} = 0.001 + 0.001\frac{\overline{T}_{dew}}{100} + 0.009Kt \tag{22}$$

Model 14: $\frac{PAR}{\overline{H}_o} = 0.011 - 0.002\frac{\overline{T}_{\min}}{\overline{T}_{\max}} + 0.402Kt + 0.055Kt^2$ (23)

Model 15: $\frac{PAR}{\overline{H}_o} = -0.001 - 0.003\frac{\overline{T}_{\min}}{\overline{T}_{\max}} + 0.448Kt + 0.005\frac{\overline{s}}{\overline{S}_o}$ (24)

3. Results and Discussion

The calculated values of monthly mean daily values of global solar radiation $(\overline{H}_m)$, sunshine hours ($\overline{s}$), dew point temperature $(\overline{T}_{dew})$, minimum temperature $(\overline{T}_{\min})$, maximum temperature $(\overline{T}_{\max})$, relative humidity $(\overline{R})$, extraterrestrial solar radiation $(\overline{H}_o)$, clearness index $(\overline{k}_t)$, characteristic day number (n), observed and predicted photosynthetically active radiation (PAR) and extraterrestrial photosynthetically active radiation (PAR_O) for calabar are presented in Tables (1-3). The observed and predicted photosynthetically active radiation (PAR) are shown in figures 1-2.

The minimum values of the monthly mean daily PAR are 5.36MJm^{-2}day^{-1}, 5.34MJm^{-2}day^{-1}, 5.33MJm^{-2}day^{-1}, 5.34MJm^{-2}day^{-1}, 5.33MJm^{-2}day^{-1}, 5.35MJm^{-2}day^{-1}, 5.34MJm^{-2}day^{-1}, 5.35MJm^{-2}day^{-1}, 5.47MJm^{-2}day^{-1}, 5.36MJm^{-2}day^{-1}, 5.35MJm^{-2}day^{-1}, 5.31MJm^{-2}day^{-1}, 5.35MJm^{-2}day^{-1}, 5.33MJm^{-2}day^{-1}, 5.32MJm^{-2}day^{-1} and 5.33MJm^{-2}day^{-1} for observed and predicted (models) irradiance respectively and they occur within the month of August. This range of values (5.32-5.47MJm^{-2}day^{-1}) are within what is expected of a tropical site [9, 18]. This is the month that is characterized by heavy rainfalls. It is pertinent to also state here that from the records of temperature readings observed during the same period, August has low monthly mean daily temperature, high monthly mean dew point temperature and relative humidity (Table 1). These occurrences could be attributed to the wet atmosphere and the presence of clouds. These factors attenuate PAR through absorption by the precipitable water vapour and through reflection and absorption by clouds [25, 26]. The same trend was observed by [9] in Ilorin, Nigeria.

The maximum values of the monthly mean daily PAR are 7.85MJm^{-2}day^{-1}, 7.85MJm^{-2}day^{-1}, 7.83MJm^{-2}day^{-1}, 7.85MJm^{-2}day^{-1}, 7.84MJm^{-2}day^{-1}, 7.86MJm^{-2}day^{-1}, 7.85MJm^{-2}day^{-1}, 7.85MJm^{-2}day^{-1}, 7.93MJm^{-2}day^{-1}, 7.86MJm^{-2}day^{-1}, 7.85MJm^{-2}day^{-1}, 7.82MJm^{-2}day^{-1}, 7.85MJm^{-2}day^{-1}, 7.84MJm^{-2}day^{-1}, 7.82MJm^{-2}day^{-1} and 7.83MJm^{-2}day^{-1} for observed and predicted (models) radiation respectively and they occur within the month of November. These range of values (7.83-7.93MJm^{-2}day^{-1}) are within what is expected of a tropical site [9, 18] but the month of occurrence (November) is not expected because of the harmattan season when aerosol mass loading greatly reduces the intensity of PAR.

The mean monthly values of 6.35MJm^{-2}day^{-1}, 6.35MJm^{-2}day^{-1}, 6.33MJm^{-2}day^{-1}, 6.35MJm^{-2}day^{-1}, 6.34MJm^{-2}day^{-1}, 6.35MJm^{-2}day^{-1}, 6.35MJm^{-2}day^{-1}, 6.35MJm^{-2}day^{-1}, 6.34MJm^{-2}day^{-1}, 6.35MJm^{-2}day^{-1}, 6.35MJm^{-2}day^{-1}, 6.32MJm^{-2}day^{-1}, 6.35MJm^{-2}day^{-1}, 6.35MJm^{-2}day^{-1}, 6.32MJm^{-2}day^{-1} and 6.33MJm^{-2}day^{-1} for observed and predicted (model) PAR respectively and they occur within the months of March – September for the rainy season. This is because, primarily, because the absorption of PAR in the intend portion of the solar spectrum is enhanced leading to reduction in the PAR under cloudy skies. Also with the movement of the Inter-Tropical Convergence Zone (ITCZ) into the Northern hemisphere, the rain-bearing South westerlies prevail as far inland as possible to bring rainfall during the rainy season. The implication is that there is a prolonged rainy season in the far South (Calabar), while the far North undergoes long dry periods annually. These values are within the range of what is expected of a tropical site [9, 18]. Similar characteristics of diurnal pattern of PAR was observed by [27] in Ilorin, Nigeria.

The mean monthly values of 7.43MJm^{-2}day^{-1}, 7.43MJm^{-2}day^{-1}, 7.41MJm^{-2}day^{-1}, 7.42MJm^{-2}day^{-1}, 7.42MJm^{-2}day^{-1}, 7.43MJm^{-2}day^{-1}, 7.42MJm^{-2}day^{-1}, 7.43MJm^{-2}day^{-1}, 7.46MJm^{-2}day^{-1}, 7.43MJm^{-2}day^{-1}, 7.43MJm^{-2}day^{-1}, 7.40MJm^{-2}day^{-1}, 7.43MJm^{-2}day^{-1}, 7.42MJm^{-2}day^{-1}, 7.40MJm^{-2}day^{-1} and 7.41MJm^{-2}day^{-1} for observed and predicted PAR respectively and they occur within the months of October – February for the dry season at Calabar. This is because cloudiness conditions occurred frequently during the dry season. This could be also attributed to influence of the Inter-Tropical Convergence Zone (ITCZ), producing Tropical Continental (TC) associated with dry and dusty North-East winds (easterlie) which blow from the Sahara desert and finally prevail over Nigeria, thus producing the dry season conditions. These values are within the range of what is expected of a tropical site [9, 18]. Similar characteristics of diurnal pattern of PAR was observed by [27] in Ilorin, Nigeria. The annual mean values of 6.76MJm^{-2}day^{-1}, 6.77MJm^{-2}day^{-1}, 6.74MJm^{-2}day^{-1}, 6.76MJm^{-2}day^{-1}, 6.75MJm^{-2}day^{-1}, 6.77MJm^{-2}day^{-1}, 6.76MJm^{-2}day^{-1}, 6.77MJm^{-2}day^{-1}, 6.76MJm^{-2}day^{-1}, 6.77MJm^{-2}day^{-1}, 6.76MJm^{-2}

175 ^{2}day^{-1}, 6.73MJm^{-2}day^{-1}, 6.77MJm^{-2}day^{-1}, 6.76MJm^{-2}day^{-1}, 6.74MJm^{-2}day^{-1} and 6.75MJm^{-2}day^{-1} for observed and
176 predicted PAR respectively. These ranged (6.73-6.77MJm^{-2}day^{-1}) values are within what is expected of a
177 tropical site [9, 18]. Similar values of mean characteristics of diurnal pattern of PAR was registered by [9] in
178 Ilorin, Nigeria.
179
180

181 **Table 1: Monthly Mean Daily Values of Global Solar Radiation $(\overline{H}_m)$, Sunshine Hours ($\overline{S}$), Dew Point**
182 **Temperature $(\overline{T}_{dew})$, Minimum Temperature $(\overline{T}_{\min})$, Maximum Temperature $(\overline{T}_{\max})$, Relative Humidity**
183 **$(\overline{R})$, Extraterrestrial Solar Radiation $(\overline{H}_o)$, Clearness Index $(\overline{k}_t)$, Characteristic Day Number (N),**
184 **Observed Photosynthetically Active Radiation (PAR) and Extraterrestrial Photosynthetically Active**
185 **Radiation (PAR_O), for Calabar (2000-2013).**

Month	$\overline{H}_m$ (MJm^{-2}day)	$\overline{H}_0$ (MJm^{-2}day)	$\overline{k}_t$	$\overline{S}$ (hrs)	$\overline{S}_o$ (hrs)	$\overline{T}_{dew}$ (^{o}C)	$\overline{T}_{\min}$ (^{o}C)	$\overline{T}_{\max}$ (^{o}C)	$\overline{R}$	PARo (MJm^{-2}day^{-1})	PAR (MJm^{-2}day^{-1})	N
JAN	15.36	34.27	0.4482	7.7	11.72	21.21	21.91	34.25	72.21	13.71	6.91	17
FEB	17.10	36.05	0.4743	8.3	11.84	21.99	23.75	34.85	71.71	14.42	7.70	45
MAR	15.72	37.51	0.4191	8.3	11.97	22.56	23.96	34.78	76.79	15.00	7.07	74
APR	15.21	37.48	0.4058	8.1	12.11	22.95	23.71	34.11	81.14	14.99	6.84	105
MAY	15.12	36.28	0.4170	8.5	12.22	23.94	23.35	31.22	83.29	14.51	6.80	135
JUN	14.00	35.31	0.3965	8.4	12.28	23.84	22.81	32.53	88.64	14.12	6.30	161
JUL	12.21	35.65	0.3425	8.7	12.25	22.36	22.20	31.54	90.14	14.26	5.49	199
AUG	11.90	37.07	0.3195	9.2	12.11	23.45	22.36	31.54	88.00	14.83	5.36	239
SEP	14.60	37.25	0.3919	9.0	12.12	21.49	22.49	31.71	90.00	14.90	6.57	261
OCT	15.58	36.15	0.4310	9.0	11.87	20.94	22.73	32.11	85.93	14.46	7.01	292
NOV	17.44	34.34	0.5079	8.8	11.76	21.79	24.50	32.54	83.00	13.74	7.85	322
DEC	16.12	33.44	0.4821	8.5	11.71	20.91	23.06	32.92	80.07	13.38	7.25	347

186

187

Table 2: Monthly, Average, Dry Season. Rainy Season and Sum of Mean Daily Values of Observed (OBS) and Predicted (Models) Photosynthetically Active Radiation (PAR) for Calabar (2000-2013).

Months	OBS PAR ($MJm^{-2}day^{-1}$)	Model 1 ($MJm^{-2}day^{-1}$)	Model 2 ($MJm^{-2}day^{-1}$)	Model 3 ($MJm^{-2}day^{-1}$)	Model 4 ($MJm^{-2}day^{-1}$)	Model 5 ($MJm^{-2}day^{-1}$)	Model 6 ($MJm^{-2}day^{-1}$)	Model 7 ($MJm^{-2}day^{-1}$)	Model 8 ($MJm^{-2}day^{-1}$)	Model 9 ($MJm^{-2}day^{-1}$)	Model 10 ($MJm^{-2}day$)
JAN	6.91	6.92	6.89	6.90	6.90	6.91	6.90	6.92	6.90	6.92	6.91
FEB	7.70	7.70	7.67	7.69	7.68	7.69	7.69	7.70	7.72	7.70	7.70
MAR	7.07	7.08	7.05	7.07	7.06	7.07	7.07	7.08	7.03	7.08	7.08
APR	6.84	6.85	6.82	6.84	6.84	6.84	6.84	6.85	6.80	6.85	6.84
MAY	6.80	6.81	6.78	6.81	6.80	6.81	6.80	6.81	6.75	6.81	6.80
JUN	6.30	6.31	6.28	6.30	6.29	6.30	6.30	6.30	6.24	6.30	6.29
JUL	5.49	5.51	5.49	5.50	5.49	5.51	5.50	5.51	5.54	5.51	5.50
AUG	5.36	5.34	5.33	5.34	5.33	5.35	5.34	5.35	5.47	5.36	5.35
SEP	6.57	6.58	6.55	6.58	6.56	6.57	6.57	6.58	6.51	6.57	6.57
OCT	7.01	7.02	6.99	7.02	7.00	7.01	7.01	7.02	6.95	7.01	7.02
NOV	7.85	7.85	7.83	7.85	7.84	7.86	7.85	7.85	7.93	7.86	7.85
DEC	7.25	7.26	7.23	7.25	7.24	7.26	7.25	7.26	7.27	7.26	7.25
AVE	6.76	6.76	6.74	6.76	6.75	6.77	6.76	6.77	6.76	6.77	6.76
RAINY	6.35	6.35	6.33	6.35	6.34	6.35	6.35	6.35	6.34	6.35	6.35
DRY	7.43	7.43	7.41	7.42	7.42	7.43	7.42	7.43	7.46	7.43	7.43
SUM	81.15	81.21	80.92	81.16	81.05	81.18	81.12	81.12	81.12	81.12	81.16

Table 3: Monthly, Average, Dry Season. Rainy Season and Sum of Mean Daily Values of Observed (OBS) and Predicted (Models) Photosynthetically Active Radiation (PAR) for Calabar (2000-2013).

Months	OBS PAR ($MJm^{-2}day^{-1}$)	Model 11 ($MJm^{-2}day^{-1}$)	Model 12 ($MJm^{-2}day^{-1}$)	Model 13 ($MJm^{-2}day^{-1}$)	Model 1 4 ($MJm^{-2}day^{-1}$)	Model 1 5 ($MJm^{-2}day^{-1}$)
JAN	6.91	6.88	6.91	6.91	6.89	6.89
FEB	7.70	7.66	7.69	7.69	7.67	7.68
MAR	7.07	7.04	7.07	7.07	7.04	7.06
APR	6.84	6.82	6.84	6.84	6.81	6.82
MAY	6.80	6.78	6.81	6.81	6.77	6.79
JUN	6.30	6.27	6.30	6.30	6.27	6.28
JUL	5.49	5.47	5.50	5.50	5.48	5.49
AUG	5.36	5.31	5.35	5.33	5.32	5.33
SEP	6.57	6.54	6.58	6.57	6.54	6.56
OCT	7.01	6.98	7.02	7.01	6.98	7.00
NOV	7.85	7.82	7.85	7.84	7.82	7.83
DEC	7.25	7.23	7.26	7.25	7.23	7.24
AVE	6.76	6.73	6.77	6.76	6.74	6.75
RAINY	6.35	6.32	6.35	6.35	6.32	6.33
DRY	7.43	7.40	7.43	7.42	7.40	7.41
SUM	81.15	80.81	81.19	81.11	80.83	80.97

Table 4: Statistical Results for the Validation of the Models of Predicted (models) Photosynthetically Active Radiation PAR in terms of their Capability for Estimating the Photosynthetically Active Radiation for Calabar (2000-2013).

Locations	*a*	*b*	*c*	d	*R*	R^2	A-R^2
Model 1	0.001	0.448			0.999	0.998	0.996
Model 2	0.009	0.406	0.050		0.999	0.998	0.996
Model 3	-0.002	0.448	0.004		0.999	0.998	0.996
Model 4	0.002	1.119			0.999	0.998	0.996
Model 5	0.020	1.034	0.103		0.999	0.998	0.996
Model 6	-0.003	1.120	0.007		0.999	0.998	0.996
Model 7	0.005	-0.002	1.118		0.999	0.998	0.996
Model 8	0.253	-0.022	1.326		0.998	0.996	0.995

Model 9	0.025	-0.003	1.025	0.111	0.999	0.998	0.996
Model 10	0.001	-0.008	0.014	1.114	0.999	0.998	0.996
Model 11	0.002	0.003	1.120		0.999	0.998	0.996
Model 12	-0.008	0.016	0.009	1.121	0.999	0.998	0.996
Model 13	0.001	-0.001	0.448		0.999	0.998	0.996
Model 14	0.011	-0.002	0.402	0.055	0.999	0.998	0.996
Model 15	-0.001	-0.003	0.448	0.005	0.999	0.998	0.996

Where *R* is the coefficient correlation of the linear regression of observed versus model's predictions of photosynthetically active radiation, R^2 is the coefficient of determination, A-R^2 is the adjusted value coefficient of determination, a is the intercept, b c and d are slope and the units of R, R^2 and A-R^2 are in $MJm^{-2}day^{-1}$

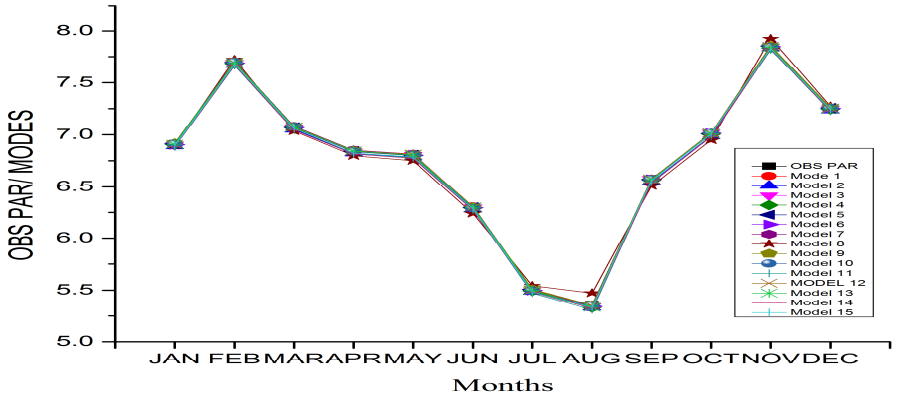

Figure 1: Comparison between the observed (OBS) and predicted (MODELS) of PAR in $MJm^{-2}day^{-1}$ for Calabar in all conditions against month

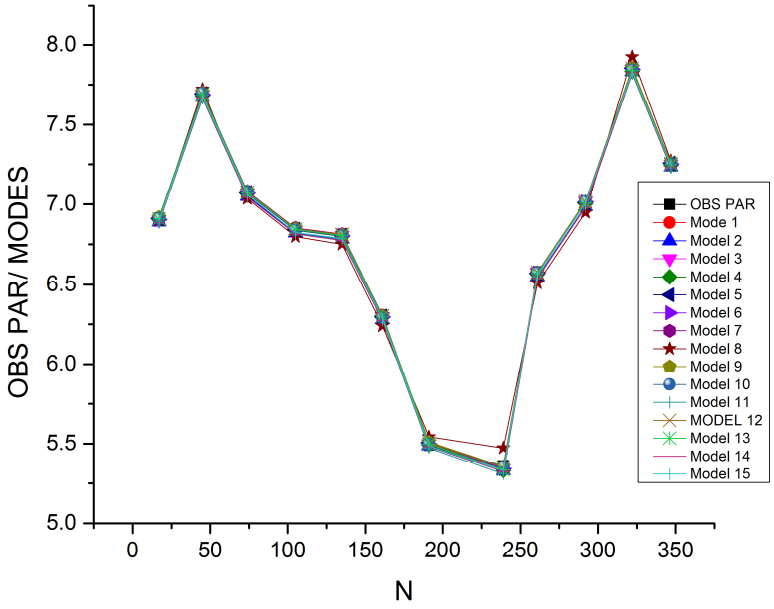

Figure 2: Comparison between the observed (OBS) and predicted (MODELS) of PAR in $MJm^{-2}day^{-1}$ for Calabar in all conditions against Characteristic Day Number (N)

In order to test the strength of the relationship between the observed and predictive models values, coefficient of correlation, R is used to test the linear relationship between observed and predicted (models) values. The value of R is between -1.0 and +1.0, the + and – signs are used for positive linear correlations and negative linear correlations. Coefficient of determination, R^2 is most often seen as a number between 0.0 and 1.0, used to describe how well a regression line fits a set of data. R^2 near 1.0 indicates that a regression line fits the data well, while an R^2 closer to 0.0 indicates that a regression line does not fit the data very well. While A-R^2 is used to check if the model is fit for generalization. The intercepts a, ranging from -0.001-0.253 and the slope(s) b, ranging from -0.001-1.119, c, 0.004-1.118, d, 0.005-1.112 of the linear regression of the observed and predicted (models) values of PAR were obtained from the correlation. These values are comparable to the values obtained in literature [28, 29, 30]. The correlation coefficient (R) of 0.998 – 0.999 exist between the explanatory variables (monthly mean daily values of the relative humidity, relative sunshine hours, extraterrestrial global solar radiation, extraterrestrial PAR, dew point temperature as well as the relative ambient temperatures) and the daily mean monthly PAR, indicating that there is high positive correlation between the observed and model's predictions values of PAR. However, this range of values are comparable to 0.994-0.998 recorded in Brazil by [30]; range of 0.84-0.97 reported in Southern Iran by [29]; 0.937-0.976 recorded by [31] in Spain and 0.994-0.999 registered by [29] in Amazon region of South America. The values of coefficient of determination (R^2) ranged from 0.996 – 0.998 implying that 99.6% to 99.8% of explanatory variables can be accounted using PAR. These values is in agreement with 70.6-94.1% repoted by [29] in Southern Iran; 87.8-95.3% reported by [31]; 98.8-0.99.8% registered by [29] in Amazon region of South America as well as 98.8-99.6% reported by [30] in Brazil. The estimated value of adjusted coefficient of determination of 0.995–0.996 from the models' predictions indicating that they are fit for making generalization in any location across the globe. Table 4 contains summary of various linear regression analysis obtained from the models' predictions at Calabar in Nigeria. A close look at figure 1 shows how the predicted (model) values fit in well with the observed PAR confirming that the variables used in estimating PAR at Calabar are good atmospheric estimators except model 8 that had little deviation from the observed.

3.1 Model Performance

In order to validate the predictions of the developed models, three statistical indicators were used to determine the performance of the predicted models. Willmott [32] developed a statistical relation called index of agreement, d, that is a dimensionless index bounded between 0 and 1. This index is a better measure of the model performance than the correlation statistics such as R and is defined as:

$$d = 1 - \left[\frac{\sum_{i=1}^{n} \left(P_i - O_i \right)^2}{\sum_{i=1}^{n} \left(\left| P_i - O_{ave} \right| + \left| O_i - O_{ave} \right| \right)^2} \right] \quad (25)$$

Where O_i represents summation of observed values of PAR, P_i represents summation of predicted (models) values of PAR, O_{ave} represents average values of observed PAR, n being the total number of observation. Nash-Sutcliffe Efficiency (NSE) scheme was also used to test the efficiency of the developed models. The efficiency, E, proposed by Nash and Sutcliffe [33] is defined according Krause et al. [34] as one minus the sum of the absolute squared differences between the predicted and observed values normalized by the variance of the observed values during the period of investigation. NSE can be determined using the relationship:

$$NSE = 1 - \left[\frac{\sum_{i=1}^{n} \left(O_i - P_i \right)^2}{\sum_{i=1}^{n} \left(O_i - O_{ave} \right)^2} \right] \quad (26)$$

Where all symbols retain their usual meaning as in equation (25). According to Willmott [32] both NSE and index of agreement, d, shows how well the plot of observed versus simulated data fits the 1:1 line. They range from -∞ and 1.0 (1 inclusive), with NSE or d =1 being the optimal value. The value between 0.0 and 1.0 are, generally, considered as acceptable levels of performance and values ≤ 0.0 indicates that the average observed value is a better predictor than simulated value, which indicates unacceptable performance. Adekunle and Emmanuel [35] suggested chi-square (χ^2) is another measure to test the performance of the developed models. The chi-square (χ^2) supplies a measure of the discrepancy between the observed and predicted. If χ^2=0, the observed and the predicted values agree exactly. If χ^2 >0, they do not agree exactly. The larger the value of χ^2, the greater is the discrepancy between the observed and predicted. This statistical indicator (χ^2) is given by:

$$\chi^2 = \left[\sum_{i=1}^{n} \frac{\left(O_i - P_i \right)^2}{P_i} \right] \quad (27)$$

where all symbols retain their usual meaning as in equation (25). To determine the error in the predictive models, Willmott [32] suggested mean bias error (MBE), mean percentage error (MPE) and root mean square error (RMSE) as good statistical indicators for evaluating the error between the observed and predicted (model) values. These relations are expressed statistically as:

$$MBE = \left[\sum_{i=1}^{n} \frac{\left(O_i - P_i \right)}{n} \right] \quad (28)$$

$$MPE = \left[\sum_{i=1}^{n} \left(\frac{O_i - P_i}{O_i} \right) \times 100 \right] / n \quad (29)$$

$$RMSE = \left[\frac{1}{N} \sum_{i=1}^{n} \left(O_i - P_i \right)^2 \right]^{1/2} \quad (30)$$

Where all symbols retain their usual meaning as in equation (25). Several researchers [36, 37, 38] have recommended that a zero value for MBE is ideal. Ituen et al. [39] suggested that MBE should be close to zero for optimal efficiency of radiometric fluxes. Akpabio and Etuk [40] recommended low value of MPE for optimal performance of solar system while [39, 36, 37, 38] have recommended that a zero value for MBE is ideal and a low RMSE is desirable. From these statistical indicators in table 5, it appears that all the models perfectly predict the observed PAR from global solar radiation and some atmospheric parameters.

Table 5: Statistical Results for the Validation of the Predictive Models of Photosynthetically Active Radiation in terms of their Capability for Estimating the Photosynthetically Active Radiation for Calabar (2000-2013).

Models	NSE	d	χ^2	MBE	MPE	RMSE
Model 1	0.999999349	0.999999837	0.000440	-0.00005	0.00616	0.0173
Model 2	0.999990440	0.999997602	0.000654	0.01917	0.02362	0.0664
Model 3	0.999999981	0.999999995	0.000001	-0.00083	-0.00102	0.0029
Model 4	0.999998192	0.999999985	0.000123	0.00833	0.01027	0.0289
Model 5	0.999999837	0.999999959	0.000011	-0.00250	-0.00308	0.0087
Model 6	0.999998375	0.999999959	0.000370	0.00250	0.00308	0.0087
Model 7	0.999999349	0.999999837	0.000440	-0.00005	-0.00616	0.0173
Model 8	0.999998375	0.999999959	0.000370	0.00260	0.00308	0.0087
Model 9	0.999999349	0.999999837	0.000440	-0.00005	-0.00616	0.0173
Model 10	0.999999981	0.999999995	0.000001	-0.00083	-0.00103	0.0029
Model 11	0.999979110	0.999994753	0.001431	0.02833	0.03491	0.0981
Model 12	0.999999710	0.999999927	0.000020	-0.00333	-0.00411	0.0116
Model 13	0.999999710	0.999999927	0.000020	0.00333	0.00041	0.0115
Model 14	0.999981495	0.999995354	0.001267	0.02667	0.03286	0.0924
Model 15	0.999994146	0.999998532	0.000400	0.01500	0.01848	0.0520

Where NSE is the Nash-Sut Cliffe equation, MBE is the mean bias error, RMSE is root mean square error, MPE is the mean bias error, χ^2 is the chi square, d is the index of agreement and all units are in $MJm^{-2}day^{-1}$

4. Conclusions

Higher mean value of 7.43 $MJm^{-2}day^{-1}$ is observed during dry season from the months October-February while in rainy season, the mean values of 6.35 $MJm^{-2}day^{-1}$ is lower with decreasing sequence from March-September South- in Calabar, South-South climatic zones. This evidence variation is due to the movement of the ITCZ into the Northern hemisphere, the rain-bearing South westerlies prevail as far inland as possible to bring rainfall during the rainy season. This result in prolonged rainy season in the far South, while the far North undergoes long dry period's annually. The total and average amount of the radiometric fluxes PAR received in Calabar are 81.15$MJm^{-2}day^{-1}$ and 6.76 $MJm^{-2}day^{-1}$ simultaneously. This indicates that crops in Calabar have a high potential for PAR utilization any month of the year provided other climatic parameters are favourable.

From the sets of the statistical indicators used in determining the performance of the models (table 5), model 3 and 10 record the highest index of agreement, Nash-Sucliffe Equation and lowest values of chi-square, mean bias error, mean percentage error and root mean squares error. This suggest that the use of atmospheric parameters such as clearness index, extraterrestrial solar radiation and relative sunshine duration to produce robust estimates of PAR for model 3 and clearness index, extraterrestrial PAR, relative humidity and relative sunshine duration for model 10 are recommended for estimating PAR at Calabar. However, model 11 registered the lowest index of agreement, Nash-Sucliffe Equation and highest values of chi-square, mean bias error, mean percentage error and root mean squares error. This we suggest that for selecting the weakest empirical model in a set of model for a radiometric fluxes, this tread is recommended. From the findings, the use of atmospheric parameters such as clearness index, extraterrestrial PAR and relative humidity may be used for estimating PAR at Calabar if there is no meteorological parameters available. In figure 1, it could be observed that all the atmospheric parameters used in modelling and estimating PAR fit in well with the observed PAR except model 8 that had the highest deviation from the observed and other models. This confirms that extraterrestrial PAR, relative humidity and clearness are meteorological parameters are not good atmospheric parameters for estimating PAR at Calabar from the month of March-December. From table 4 and 5, it could be observed that index of agreement, d, appears to be a better measure of testing model performance than correlation statistics such as correlation coefficient, r, and Nash-Sucliffe Equation, NSE. Therefore, the proposed models could be used to estimate PAR at Calabar and other locations with similar climatological conditions across the globe.

References

[1] K.J. McCree, Test of current definitions of photosynthetically active radiation against leaf photosynthesis data. Agric. For. Meteorol. 10 (1972) 443–453.

[2] J. Ross, M. Suler, Sources of errors in measurements of PAR. Agric. and For. Meteorol., 100 (2000) 103-125

[3] J.G. Williams, Small variation in the photosynthetically active radiation of solar radiation on clear days. J. Arch. Meteor. Geophs. Bioclim. 33 (1976) 89-98

[4] M. Tsubo, S. Walker, Relationships between photosynthetically active radiation and clearness index at Bloemfontein, South Africa. Theor. Appl. Climatol., 80 (2005) 17–25, DOI:10.007/s00704-0080-5

[5] P. Moon, Proposed standard solar radiation curves for engineering use. J. Franklin Inst., 230 (1940) 583-618.

[6] J.L. Monteith, Principle of Environmental Physics, First ed. Edward Arnold, London, 1973.

[7] T.A. Howell, D.W. Meek, J.L. Hatfield, Relationship of photosynthetically active radiation to shortwave radiation in the San Joaquin Valley. Agric. For. Meteorol. 28 (1983)157–175, DOI:10.10160021571(83)90005-5.

[8] D.W. Meek, J.L. Hatfield, J.L. Howell, T.A. Idso, S.E. Reginato, R.J. A generalized relationship between photosynthecally active radiation and solar radiation. Agron. J., 76 (1984) 939-945

[9] S.O. Udo, T.O. Aro, Global PAR related to global solar radiation for Central Nigeria. Agric. For. Meteorol., 97 (1999) 21–31, DOI:10.1016S0168-1923(99)00055-6

[10] D.A. Finch, W.G. Bailey, L.J.B. McArthur, M. Nasitwitwi, Photosynthetically active radiation regmes in a South African savanna environment. Agric. and For. Meteoro., 122 (2004) 229-238

[11] C.R. Rao, Photosynthetically-active components of global solar radiation: Measurements and model computations. Arch. Meteorol. Geophys. Bioclim., Set. B, 33 (1984) 89-98.

12] G. Papaioannou, N. Papanikolaou, D. Retails, Relationships of photosynthetically-active radiation and shortwave irradiance. Theor. Appl. Climatol., 48 (1993) 23-27, DOI:10.1007/bf00864910

[13] C.P. Jacovides, F.S. Timvios, G. Papaioannou, D.N. Asimakopoulos, C.M. Theofilou.. Ratios of PAR to broadband solar radiation measured in Cyprus. Agric. and For. Meteor., 121 (2004) 135-140, DOI:10.1007/s00704-002-0685-5

[14] R. Li, L. Zhao, Y.L. Ding, S. Wang, G.L. Ji, Monthly ratios of PAR to photosynthetically active radiation to global solar radiation measured at Northern Tibetan platean, China. Solar Ener., 84 (2010) 964-973

[15] Q. Wang, Y. Kakubari, M. Kubota, Variation of PAR to global solar radiation ratios along altitude gradient in Naeba Mountain. Theo. and Appl. Clima., 87 (2007) 239-253

[16] C.M. Britton and J.D. Dodd, Relationships of photosynthetically-active radiation and shortwave irradiance. Agric. Meteorol., 17 (1976) 1-7.

[17] G. Szeiez, Solar radiation for plant growth. J. of appl. Ecol., 11 (1984) 617-636

[18] F. Miskolczi, T.o. Aro, M. Iziomon, R.T. Pinker, Surface radiation fluxes in sub Sahel Africa, J. of Appl. Meteo., 36 (1997) 521-530.

[19] J.L. Monteith, M. Unsworth, Principle of Environmental Physics, Second ed. Edward Arnold, London, 1990.

[20] T. Bat-Oyun, M. Shinoda, M. Tsubo, Effect of cloud, atmospheric water and dust on photosynthetically active radiation in a Mongolian grassland. J. of Ari. Land, 4 (2012) 349-356

[21] J.C. Ododo, New Models for the Prediction of Solar Radiation in Nigeria, Paper presented at the 2nd OAU/STRC Conference on New, Renewable and Solar Energies, at Bamako Mali, 16 – 20, 1994.

[22] M. Igbal, An introduction to Solar Radiation, First ed. Academy Press. New York, 1983.

[23] K.N. Liou, Introduction to Atmospheric Radiation, Academy Press, New York, 1980.

[24] D.M. Gates, Biophysical Ecology, third ed. Springer-Verlag, New York, 1980.

[25] E.B. Babatunde, T.O. Aro, Characteristics Variation of total solar radiation at llorin, Nigeria. Nig. J. Sol. Ener. 9 (2001) 157 - 173.

[26] E.B. Babatunde, Solar radiation modeling for a tropical station, llorin, Nigeria. Ph.D thesis 32-34, 2001.

[27] S.O. Udo, T.O. Aro, L.E. Akpabio, Characteristics of diurnal pattern of global photosynthetically active radiation at Ilorin, Nigeria. Nigerian J. of Phy., 18 (2006) 223-226.

[28] M. Abolfazi, Estimating photosynthetically active radiation (PAR) using air temperature and sunshine duration. J. of Biod. and Environ. Scien., 4 (2014) 371-377

[29] L.J.G. Aguiar, G.R. Fischer, R.J. Ladle, A.C.M. Malhado, F.B. Justino, R.G. Aguiar, J.M.N. Costa, Modeling the photosynthetically active radiation in South West Amazonia under all sky condition. Theor. Appl. Clmatol., 2011. DOI: 10:1007/500704-011-0556-z

[30] J.E. Escobedo, E.N. Gomes, A.P. Oliveira, J. Soares, Modeling hourly and daily fractions of UV, PAR and NIR to global solar radiation under various sky conditions at Botucatn, Brazil. Appl. Energ., (2008), DOI:10.1016/j.apenergy.2008.04.013

[31] I. Alados, I. Foyo-Moreno, F.J. Olmo, L. Alados-Arboledas, F.A. Grupo, Improved estimation of diffuse Photosynthetically active radiation using two spectral models. Agric. and For. Meteorol., 111 (2002) 1-12. DOI: 10.1016/SO168-1923(02)00010-2

[32] C.J. Willmott, On the validation of models. J. Phys. And Geogr., 2 (1981)184-194

[33] J.E. Nash, J.V. Sutcliffe, River flow forecasting through conceptual models 1. A discussion of principles. J. of Hydrol.,10 (1970) 282-290

[34] P. Krause, D.P. Boyle, F. Base, Composition of different efficiency criteria for hydrological models assessment. J. Adv. Geosci., 51 (2005) 89-97

[35] A.O. Adukunle, C.O. Emmanuel, Correlation of global solar irradiance with some meteorological parameters and validation of some existing solar radiation models with measured data over selected climatic zones in Nigeria. International J. for. Inno. Educ. and Res., 1 (2014) 1-7.

[36] M. Halouani, C.T. Nguyen, D. Vongoc, Calculation of monthly average global solar radiation on horizontal surfaces using Daily Hours of Bright Sunshine, Solar Ener., 50 (1993) 247-255.

[37] H.Z. Che, G.Y. Shi, X.Y. Zhang, J.Q. Zhao, Y. Li, Analysis of sky condition using 40 years records of solar radiation data in China. Theor. and appl. Climat. 89 (2007) 83 - 94.

[38] J. Almorox, M. Benito, C. Hontoria, Estimating of Monthly Angstrom – Prescott equation coefficients from measured daily data in Toledo, Spain. Renewable Energy J., 30 (2005) 931 - 936.

[39] E.E. Ituen, N.U. Esen, S.C. Nwokolo, E.G. Udo, Prediction of global solar radiation using relative humidity, maximum temperature and sunshine hours in Uyo, in the Niger Delta Region, Nigeria. Advances in Applied Science Research, 4 (2012)1923-1937

[40] L.E. Akpabio, S.E. Etuk, Relationship between solar radiation and sunshine duration for Onne Nigeria.,Turkish J. Phys., 27 (2002) 161 - 167.